Stem Cell Research & Therapy

RESEARCH

Open Access

Hybrid endometrial-derived hydrogel and human endometrial organoids synergize for uterine regeneration in an immunocompetent murine model

María Gómez-Álvarez[1†], Clara Bueno-Fernandez[1†], Emilio Francés-Herrero[1,2], Marcos Agustina-Hernández[1], Paula Alonso-Frías[1,2], Nadaya Corpas[1], Amparo Faus[1], Ana Díaz[2], Antonio Pellicer[3], Hortensia Ferrero[1†] and Irene Cervelló[1*†]

Abstract

Background The human endometrium is a regenerative tissue essential for fertility, but pathological conditions like Asherman syndrome, endometrial atrophy, and thin endometrium can impair its function. Current therapies lack efficacy, driving demand for innovative regenerative therapies. In this context, endometrial-derived hydrogels and organoids have shown promise individually for tissue regeneration, but their combined therapeutic potential has not been previously evaluated in vivo. This study explores a dual regenerative strategy combining a hybrid hydrogel — composed of synthetic PuraMatrix® and endometrial extracellular matrix hydrogel — with human endometrial organoids in an immunocompetent murine model with uterine damage.

Methods Endometrial damage model was established in female C57BL/6 mice ($n=46$) via uterine injury using 70° ethanol. After 4 days of endometrial damage, human endometrial organoids were co-injected with the hybrid hydrogel into the uterine horns. Two weeks post-injection, a subset of mice ($n=25$) was sacrificed for biocompatibility, histological, and transcriptomic analyses. Functional recovery of the endometrium was assessed in the remaining animals ($n=21$) through fertility outcome evaluation. For endometrial regeneration analyses, normally distributed data were analyzed by one-way ANOVA and Tukey's multiple comparisons, while non-normally distributed data were analyzed by the Kruskal–Wallis test with Dunn's multiple comparisons. For fertility outcomes, *t*-test or Mann–Whitney U tests for 2-by-2 comparisons were performed.

†María Gómez-Álvarez and Clara Bueno-Fernandez have contributed equally to this work and should be considered joint first authors.

†Hortensia Ferrero and Irene Cervelló have contributed equally to this work and should be considered joint senior authors.

*Correspondence:
Irene Cervelló
irene.cervello@ivirma.com

Full list of author information is available at the end of the article

© The Author(s) 2026. **Open Access** This article is licensed under a Creative Commons Attribution-NonCommercial-NoDerivatives 4.0 International License, which permits any non-commercial use, sharing, distribution and reproduction in any medium or format, as long as you give appropriate credit to the original author(s) and the source, provide a link to the Creative Commons licence, and indicate if you modified the licensed material. You do not have permission under this licence to share adapted material derived from this article or parts of it. The images or other third party material in this article are included in the article's Creative Commons licence, unless indicated otherwise in a credit line to the material. If material is not included in the article's Creative Commons licence and your intended use is not permitted by statutory regulation or exceeds the permitted use, you will need to obtain permission directly from the copyright holder. To view a copy of this licence, visit http://creativecommons.org/licenses/by-nc-nd/4.0/.

Results Histological and molecular analyses revealed that the therapy improved endometrial thickness, gland density, and vascularization, and reduced fibrosis and ferroptosis, aligning tissue characteristics closer to healthy controls. However, fertility outcomes were not fully restored, potentially due to the persistence of the synthetic component of the hybrid hydrogel. Thus, further studies are needed to confirm complete hydrogel resorption and its impact on fertility restoration.

Conclusions In conclusion, this study demonstrates the biocompatibility and regenerative potential of human endometrial organoids delivered within the hybrid hydrogel, highlighting a promising strategy for endometrial regeneration.

Keywords Hybrid hydrogel, Human endometrial organoids, Endometrial pathology, *In vivo* regeneration

Background

The human endometrium is the innermost layer of the uterus, undergoing tissue regeneration every menstrual cycle [1]. This dynamic tissue consists of luminal and glandular epithelia surrounded by stroma and blood vessels. Additionally, the endometrium is supported by a niche of epithelial and stromal stem cells that contribute to its regenerative capacity [2]. This remarkable ability to renew itself is essential for reproductive success, but pathological changes in the endometrial structure and function can lead to infertility. Endometrial diseases, such as Asherman syndrome (AS), endometrial atrophy (EA), and thin endometrium (TE) are characterized by fibrosis, glandular loss, and impaired vascularization, which significantly reduce the chances of a successful pregnancy [3]. The limited effectiveness of current treatments, including hormonal therapies and surgical interventions, highlights the need for innovative therapies to restore the endometrial structure and function [4].

In recent years, regenerative medicine has emerged as a promising strategy for endometrial repair [4]. Within this field, bioengineering approaches, particularly the use of hydrogels, have been explored for their potential to support tissue regeneration [5]. Natural hydrogels, such as those derived from the endometrial extracellular matrix (EndoECM), can be obtained by the decellularization of the endometrium to remove cellular components while preserving the native proteins and bioactive factors necessary for tissue remodelling [6]. On the other hand, synthetic hydrogels, such as PuraMatrix® (PM, Corning), offer excellent biocompatibility, high mechanical stability, and durability [5, 7]. Due to its simple composition, consisting exclusively of water and $RADA_{16}$ peptide sequences, several PM-based formulations have been approved in Europe, the United States, and Japan to control intraoperative bleeding in surgical procedures [8]. $RADA_{16}$ is a peptide-based biomaterial whose acidic aqueous solution spontaneously forms an extracellular matrix-like three-dimensional structure [9]. While ECM-derived hydrogels retain the biochemical cues of the native endometrium, they often lack mechanical stability, whereas synthetic hydrogels offer tunable mechanical properties, good biocompatibility, low immunogenicity, and it is a good delivery vehicle for cells, drugs and factors but with limited bioactivity. Thus, a hybrid hydrogel PM + EndoECM (HG), integrating natural (EndoECM) and synthetic (PM) components, may provide an optimal platform to advance bioengineering strategies for the treatment of endometrial pathologies [10]. Unlike other hybrid biomaterials have been described in the literature to enhance cellular engraftment [11], improve vascularization [12], and support long-term tissue regeneration [13], the combination of EndoECM with PM remain underexplored for the endometrial in vivo regeneration.

In addition to bioengineering, cellular therapies have shown promising results in the treatment of endometrial pathologies over the last decade [4]. One such advancement is the use of human epithelial endometrial organoids (hEOs), which are three-dimensional structures derived from epithelial progenitor cells that mimic the cellular architecture of human endometrial glands [5]. Beyond their role as in vitro models, organoids hold great potential as a cell-based therapy for endometrial regeneration, providing a biological source of endometrial progenitor cells that can be used to restore endometrial function [14, 15]. When combined with bioactive carriers such as hydrogels, organoids can preserve their three-dimensional complexity while also exhibiting improved retention at the injection site [16]. Unlike several studies have explored the use of endometrial organoids in AS/EA/TE animal models, this cellular approach requires further investigation into their efficacy and long-term impact [14, 15, 17]. Moreover, Matrigel® (Corning) remains the most commonly used hydrogel carrier, which presents notable disadvantages such as its murine tumor-derived origin, limiting its in vivo applicability [18]. Therefore, understanding how implanted organoids interact with host tissue and optimizing their delivery system is crucial for the translation of these experimental approaches into clinical treatments.

Taken together, the objective of this study is to unveil the potential of a dual synergistic approach, integrating a cellular therapy (hEOs) with a bioengineering tool (PM + EndoECM), for the restoration of endometrial

structure and function in an immunocompetent murine model of AS/EA/TE. Specifically, this investigation aims to assess endometrial regeneration through comprehensive histological and molecular analyses, while also examining the potential for fertility restoration after treatment.

Methods

Experimental design

The in vitro experiments involved the PM + EndoECM hybrid hydrogel (HG) synthesis and organoid culture (hEOs). HG was synthesized by combining extracellular matrix endometrial-derived hydrogel from decellularized porcine tissues with PM 1%. In addition, hEOs were propagated during several passages to obtain enough cell concentration for all animals. The AS/EA/TE animal model was established in 8-week-old female C57BL/6 mice ($N = 46$), via uterine injury using 70 °C ethanol. Four days after the induction of endometrial damage, HG with or without hEOs were injected into the uterine horns (named as HG and HG + hEOs conditions, respectively). After 14 days of treatment, mice were euthanized to evaluate endometrial regeneration by histological and molecular analyses or mated with males to assess fertility restoration. Figure 1 provides a description of the experimental design followed in this research.

The work has been reported in line with the ARRIVE guidelines 2.0.

Preparation of injectable hybrid endometrial-derived hydrogel

To create the natural component of the HG, the EndoECM hydrogel, porcine uterine horns were decellularized following a two-cycle protocol as previously described [19]. Briefly, 0.1% SDS and 1% Triton X-100 were perfused through the uterine artery using a peristaltic pump (Cole-Parmer Instruments, Fisher Scientific). The horns were cut transversally into 1 mm thick disks, and the endometrial tissue was manually microdissected under a stereomicroscope (SMZ800, Nikon). To remove residual DNA and detergents, the endometrial tissue was washed in PBS (10 mL/g tissue) and incubated for 1 h in DNase I solution (5 µg/mL, D5025, Sigma-Aldrich) at room temperature (RT). Next, the porcine endometrium was flash-frozen in a mortar with liquid N_2, milled manually, and lyophilized (Lyoquest-85, Telstar, Valencia's Polytechnic University) over 96 h at 20 Pa. This lyophilized powder was digested with 0.01 M HCl (H1758, Sigma-Aldrich) and 0.1% pepsin (P7000, Sigma-Aldrich), and finally neutralized with 10% (v/v) 0.1 m NaOH (S8045, Sigma-Aldrich), 11.11% (v/v) 10X PBS (P5493, Sigma-Aldrich), and 1X PBS until the desired concentration (8.25 mg/mL) was obtained. The resulting EndoECM hydrogel was stored at − 80 °C until use.

For the synthetic component, the PuraMatrix hydrogel (PM, 10 mg/mL, 10255252, Fisher Scientific) was first subjected to bath sonication for 30 min to reduce its viscosity. Then, a 1% PM solution was mixed in a 1:1 ratio with the EndoECM hydrogel (8.25 mg/mL), yielding the HG hybrid formulation with final concentrations of 5 mg/mL PM and 4.12 mg/mL EndoECM. To ensure uniformity, the mixture underwent an additional 10-min sonication before being stored at 4 °C until further use.

Long-term culture of human endometrial organoids and their Preparation for in vivo experiments

This study was approved by the Ethical Committee of the Hospital Universitari I Politècnic La Fe (2021-162-1, Valencia, Spain) and conducted in accordance with the institutional and international guidelines for the use of human-derived samples. Endometrial biopsies were processed following established protocols to generate hEOs [20]. For this study, multiple cryopreserved vials of hEOs (passage 10), originating from the same endometrial biopsy and stored in our organoid biobank, were thawed following an established protocol [20]. Briefly, the frozen vials were retrieved from liquid nitrogen and thawed in a 37 °C water bath for 2 min. The cell suspension was then transferred to a 15 mL tube containing 10 mL Advanced DMEM/F-12 (Thermo Fisher Scientific, 12634010) and centrifuged (600 g, 6 min). After centrifugation, the supernatant was removed, and the resulting pellet was resuspended in 1 mL of Advanced DMEM/F-12. A second centrifugation step (600 g, 6 min) was performed, after which the pellet was reconstituted in a mixture of 15% Advanced DMEM/F-12 and 85% ice-cold Matrigel (Corning, 354234). Matrigel drops (20 µL) were plated onto 48-well plates (Corning TM, 3548) and incubated at 37 °C for 30 min to allow gelation. Subsequently, 250 µL of organoid expansion medium (ExM) supplemented with Y-27632 was added [20]. After three days, the culture medium was replaced with ExM medium lacking Y-27632 supplementation. Organoids were cultured through multiple passages to generate sufficient stock for the subsequent experiments.

On the day of injection, hEOs (passage 15) were harvested from the 48-well plates. Specifically, ExM was removed, and 250 µL of VitroGel® Organoid Recovery Solution (TheWell Bioscience, MS04-100) was added to each well. Drops were scratched from the plate with the pipette tip, transferred to a tube and gently agitated for 2 min to dissolve the Matrigel. Next, samples were centrifuged (600 g, 5 min), the supernatant was discarded, and the pellet was resuspended in 1 mL of Advanced DMEM/F-12. Organoids were partially dissociated by repeated pipetting (80 times) before homogenized with the HG hydrogel and maintained on ice until injection into the AS/EA/TE animal model.

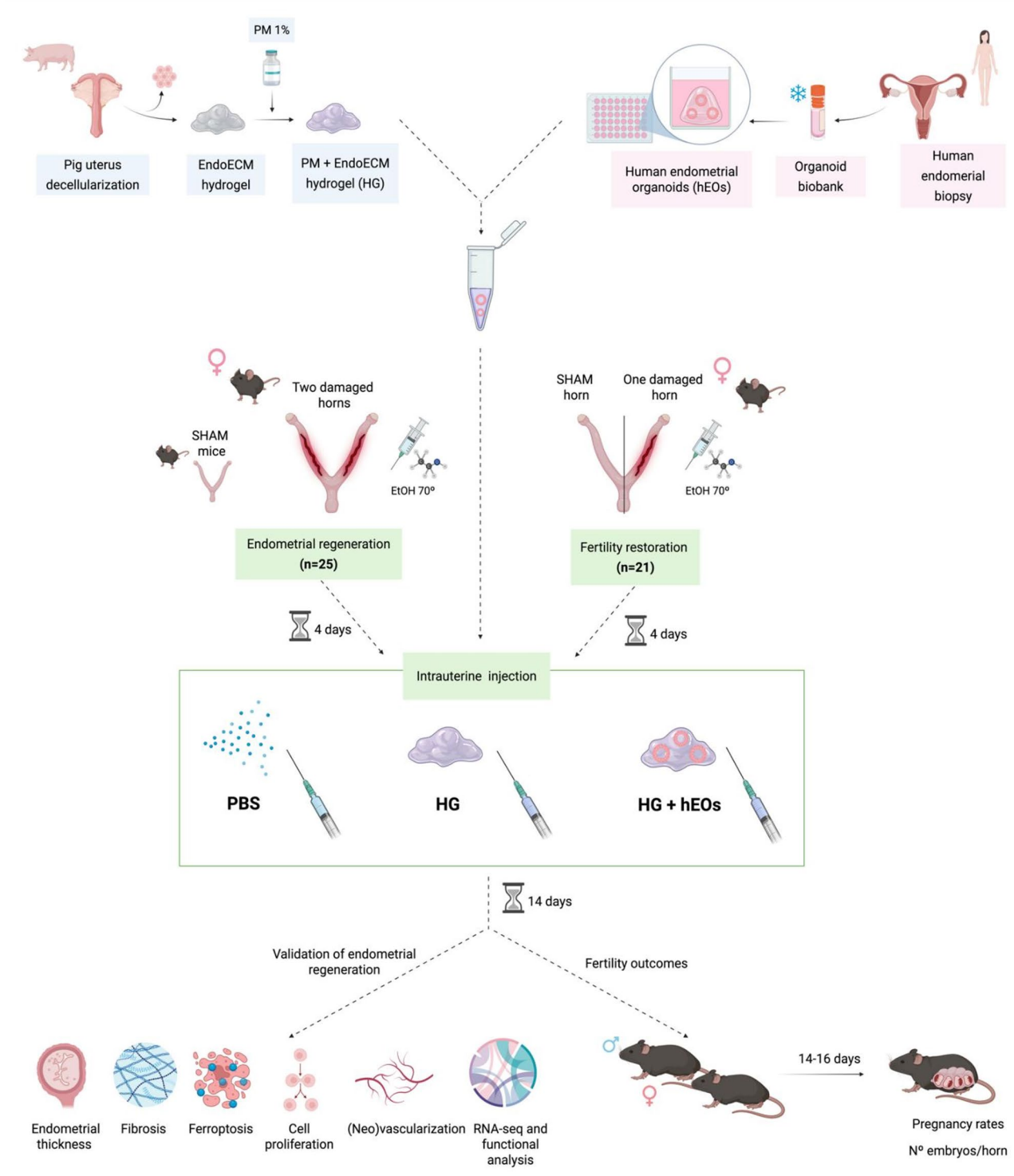

Fig. 1 Experimental design. The hybrid hydrogel (HG) was synthesized by combining decellularized porcine endometrial extracellular matrix (EndoECM) with 1% PM. Human endometrial organoids (hEOs) were cultured, expanded, and incorporated into the hydrogel. Endometrial injury was induced in C57BL/6 female mice ($n = 46$) with 70° ethanol, and then they were divided into two groups: one for endometrial regeneration ($n = 25$), where both uterine horns were damaged and a SHAM group was included; and another for fertility restoration ($n = 21$), where only one horn was damaged while the other remained intact (SHAM). Four days post-injury, damaged horns were treated with PBS, HG, or HG + hEOs. Fourteen days later, endometrial regeneration was evaluated histologically and molecularly, or fertility restoration was assessed by mating. *HG* PM + EndoECM, *EtOH* ethanol

Animal care

All animal procedures complied with Directive 2010/63/EU and were approved by the Generalitat Valenciana (2024-VSC-PEA-0110, 2024-VSC-PEA-0225). A total of 46 six-week-old female C57BL/6 mice and 11 male C57BL/6 mice were sourced from Charles River Laboratories (Écully, France). Additionally, 12 six-week-old female C57BL/6 mice were included to evaluate the effect of PM alone in fertility outcomes. Mice were housed in cages under controlled environmental conditions, including a 12-hour light/dark cycle, regulated temperature, and relative humidity, with *ad libitum* access to food and water. At specific time points throughout the study, animals were weighted by using a conventional scale. All experiments were conducted at the animal facilities of the Central Research Unit, Faculty of Medicine, Universitat de València (Valencia, Spain).

Establishment of a murine model of endometrial damage

Endometrial injury was induced by intrauterine injection of 70 °C ethanol for 3 min, as we have described in previous publications [16, 21]. Briefly, animals were anesthetized, and the uterine horns were clamped at the upper and lower regions to confine the ethanol instillation to the targeted area. After injury induction, the clamps were released, and the horns were thoroughly washed with saline solution.

Female mice (n = 46) were allocated into two experimental sets: endometrial regeneration analysis and fertility recovery assessment. For the endometrial regeneration study (n = 25), a bilateral uterine injury was performed. One uterine horn was designated for histological evaluation, while the contralateral damaged horn was allocated for molecular analysis. Within this experimental set, animals were randomly distributed into four groups: SHAM (n = 6), PBS (n = 6), HG (n = 6), and HG + hEOs (n = 7). The SHAM group, neither injured nor treated, was included exclusively in this experiment to serve as a baseline control for normal endometrial conditions.

For the fertility recovery study (n = 21), a unilateral injury model was employed, leaving the contralateral horn intact as an internal positive control. In this set, animals were assigned to three experimental groups: PBS (n = 5), HG (n = 8), and HG + hEOs (n = 8). To clarify variations in fertility outcomes, two additional groups treated with PM alone (n = 12) were included: one without endometrial injury (n = 5) and one with damage (n = 7). Female mice were mated with males in a 3:1 ratio.

Four days after inducing endometrial damage, a second surgical procedure was performed to administer the treatments intrauterinely. Specifically, 50 µL of either PBS, HG, or HG supplemented with hEOs (~ 10^6 cells per horn) was directly injected into the injured endometrial wall using a 25G needle. Following the procedure, mice were sutured and maintained under standard conditions with appropriate analgesic and antibiotic treatment.

Sacrifice and sample collection

Mice were euthanized two weeks post-treatment by exsanguination under general anesthesia [isoflurane 4% (zoetisIsoFlo®, ecuphar) until loss of reflexes], followed by cervical dislocation. Then uteri and blood were harvested for subsequent analysis. One uterine horn was fixed in 4% paraformaldehyde for histological evaluation, while the contralateral horn was stored at − 80 °C for RNA sequencing and transcriptomic analysis.

Haematocrit analysis and treatment biocompatibility

To assess the biocompatibility of the treatments, blood samples were collected from the cava vein of mice designated to analyze endometrial regeneration. For each animal, 20 µL of blood was combined with 2 µL EDTA and analyzed with an Auto Haematology Analyzer – Element HT5-HESKA.

Histological analysis of endometrial regeneration

After fixation, uterine horns were dehydrated, embedded in paraffin, and sectioned into 4-µm vertical cross-sections for subsequent analysis.

Endometrial thickness and gland concentration

Endometrial parameters, including epithelial, stromal, and endometrial thickness, as well as gland concentration, were assessed from sections stained with haematoxylin and eosin (H&E) (HT20, Sigma-Aldrich). For each uterine horn, five different cross-sections (at 5x magnification) were analyzed, with five random measurements taken from each section (total 25 measurements/horn). Samples were observed under a Leica microscope (LEICA DM4000B, Leica Microsystems GmbH, Germany) and analyzed using FIJI-ImageJ software (Rasband, USA) and QuPath software version 0.5.1.

Endometrial fibrosis

Endometrial fibrosis was evaluated using Masson's Trichrome staining (MT, HT-15, Sigma-Aldrich). Specifically, three different uterine sections per mouse were analyzed (at 20x magnification), with four random 20x fields per section (total 12 fields/horn). Samples were observed under a Leica microscope and analyzed using QuPath software version 0.5.1 (Color Deconvolution plugin).

Endometrial ferroptosis

To assess ferroptosis in the murine endometrial tissue, Prussian Blue (PB) staining was performed following the manufacturer's instructions. For each uterine horn, three

different uterine sections per mouse were analyzed (at 10x magnification). Samples were examined under Leica microscope and analyzed using FIJI-ImageJ software (Rasband, USA).

Endometrial cell proliferation

Endometrial cell proliferation was assessed by immunofluorescence (IF) of Ki67 marker. Specifically, antigen retrieval was performed with 10 mM citrate buffer at pH 6.0 (20 min, 95 °C). Afterward, sections were permeabilized with 0.05% Tween (10 min, RT), blocked in 5% BSA (1 h, RT), and incubated with anti-Ki67 polyclonal antibody (1:300 dilution, ab15580; Abcam, Cambridge, MA, USA) diluted in blocking solution overnight at 4 °C. The following day, sections were incubated with Alexa Fluor 488-conjugated goat anti-rabbit IgG secondary antibody (Invitrogen, A11034, 1:500) and counterstained with DAPI (Thermo Fisher Scientific, 62 248). Images were captured using a Leica microscope. The percentage of Ki67-positive cells was quantified from four random 40x fields per uterine section by using a Leica microscope and analysing with QuPath analysis software 0.5.1.

Endometrial neovascularization

The formation of new blood vessels was evaluated using well-described protocols with slight modifications [16, 22]. Briefly, antigen retrieval in the uterine samples was performed with Tris EDTA buffer pH 9.0 (95 °C, 20 min). Then, sections were washed with PBS and incubated in Carbo-Free™ Blocking Solution (Vector Laboratories, SP-5040-125) (30 min, RT). Afterward, they were treated with 1% BSA (10 min), followed by another 20 min incubation in Carbo-Free™ Blocking Solution. To detect new blood vessels, the sections were incubated overnight at 4 °C with fluorescein-labeled Griffonia Simplicifolia Lectin I (GSL I, 1:200, FL-1101; Vector Laboratories, Burlingame, CA, USA). On the following day, sections were washed twice with PBS and incubated with alpha-smooth muscle actin (α-SMA, 1:200, C6198; Sigma-Aldrich) (30 min, RT). After a second round of PBS washing, sections were treated with Tris-buffered saline containing 0.1% Tween®20 detergent and mounted with DAPI. For vessel analysis, four 40x magnification fields per uterine horn were selected, observed under a Leica microscope, and analyzed using Image-Pro Plus (Media Cybernetics; Carlsbad, CA, USA) software. Areas positive for GSL I alone were considered as new vessels, while regions co-positive for both GSL I and α-SMA were classified as mature vessels. Neovascularization was quantified by subtracting the mature vessel area from the new vessel area per Sect [21].

Molecular analysis of endometrial regeneration

The endometrial tissue was carefully separated from the myometrium by applying gentle pressure along the uterine horns using the back of curved forceps, facilitating the expulsion of the endometrial layer [23]. Total RNA was extracted from the isolated endometrial tissue from each horn (n = 23, 2 samples were discarded due to technical problems) using the RNAeasyVR Mini Kit (74014, Qiagen, Hilden, Germany), following the manufacturer's protocol.

For mRNA library preparation, total RNA was processed using the Illumina Stranded mRNA Prep Kit (20020595, Illumina, San Diego, CA, USA). Initially, mRNA molecules were selectively purified using oligo-dT beads that bind to poly(A) tails. These fragments were then fragmented and hybridized with random hexamers to synthesize the first-strand of complementary DNA (cDNA). The second-strand cDNA was generated using deoxyuridine triphosphate (dUTP) to enable strand specificity. The resulting double-stranded cDNA was ligated to indexed adapters and subsequently enriched via polymerase chain reaction (PCR).

The resulting cDNA libraries were quantified using fluorometry and their fragment sizes were assessed with the Agilent 2100 Bioanalyzer. An equimolar pool of all samples was prepared and sequenced on the NextSeq 550 platform (Illumina, San Diego, CA, USA) using single-end 75-cycle sequencing (1 × 75 bp) with a High Output Reagent Cartridge (400 M reads).

RNA-sequencing data processing and analysis

The quality of raw RNA sequencing reads was assessed using FastQC (v0.11.9), and summary reports were generated with MultiQC (v1.27.1). Adapters and low-quality bases were trimmed using Trimmomatic (v0.39) [24]. Trimmed reads were aligned to the Mus musculus reference genome (GRCm39) using HISAT2 (v2.2.1) [25] with --dta for transcriptome-aware alignment. SAM files were converted to sorted BAM format using SAMtools (v1.21) [26]. Gene-level counts were generated with featureCounts (v2.0.3) [27] (Subread package) using the mouse genome annotation. Raw counts were processed in R (v4.3.1) using DESeq2 (v1.42.1) [28]. Low-expression genes were filtered (rowSums ≥ 10 counts in ≥ 3 samples), and data were normalized via the median-of-ratios method.

Differential expression was tested using DESeq2's negative binomial Wald test, applying Benjamini-Hochberg (FDR) correction with a threshold of $|\log2FC| > 1$ and adjusted p-value < 0.05. Gene Ontology (GO) and KEGG pathway analyses were performed using clusterProfiler (v4.10.1) [29] for gene set enrichment analysis (GSEA). ENSEMBL IDs were mapped to ENTREZIDs using org.Mm.eg.db (v3.18.0). Principal component analysis (PCA)

and hierarchical clustering were conducted on variance-stabilized transformed (VST) data using ggplot2 (v3.5.2) [30] and pheatmap (v1.0.12).

Evaluation of fertility restoration

Functional recovery of the uteri was assessed two weeks post-treatment through pregnancy outcomes following natural mating. Female mice ($n = 21$), each with a single injured/treated uterine horn, were divided into three experimental groups: PBS ($n = 5$), HG ($n = 8$), and HG + hEOs ($n = 8$). In addition, two groups treated with PM alone were also included ($n = 12$), with ($n = 7$, PM damaged) or without ($n = 5$, PM non-damaged) endometrial damage, to address inconsistencies observed in fertility outcomes. Mating was conducted using 12-week-old C57BL/6 male mice and continued for one week. Successful mating was confirmed by the presence of a vaginal plug. Fourteen to sixteen days after plug detection (E14–E16), uteri were collected to evaluate fertility outcomes.

Statistical analyses

Statistical analyses were performed using the IBM SPSS statistics software (v24.0). Outliers were detected and removed from analysis using Grubbs test. For endometrial regeneration analyses, normally distributed data were analyzed by one-way ANOVA and Tukey's multiple comparisons, while non-normally distributed data were analyzed by the Kruskal–Wallis test with Dunn's multiple comparisons. For fertility outcomes, the normality of data was checked and t-test or Mann–Whitney U tests for 2-by-2 comparisons were performed. Probability values less or equal to 0.05 ($p \leq 0.05$) were considered as statistically significant. Quantitative data were expressed as the mean value ± standard error of the mean (SEM). GraphPad Prism software v 8.3 (www.graphpad.com; La Jolla, CA, USA) was used for graphical representation. No animals were excluded from the analyses.

Results

A biocompatible biomaterial suitable for in vivo application

To monitor potential systemic effects of the treatment, mice were weighed on days 1, 3, and 14 post-treatment. No significant differences in body weight were observed between groups, indicating no adverse impact on overall health (Fig. 2). In addition, blood samples from the mice of the endometrial regeneration set ($n = 25$) were analyzed on the 14th day post-treatment. Haematocrit tests showed no pathological alterations of white blood cells, red blood cells, and platelets in any of the four conditions. When further analyze leukocytes, no differences were found in the proportion of neutrophils, lymphocytes, monocytes, eosinophils, and basophils between groups (Fig. 2). All these findings suggest that HG alone or HG + hEOs did not cause any systemic immune disorders in our immunocompetent murine model.

Histological and functional regeneration of the endometrium after treatment

Fourteen days after treatment, one uterine horn per animal was harvested for comprehensive histological analysis. Endometrial regeneration was evaluated through the quantification of endometrial thickness, gland density, fibrosis, cellular proliferation, and neovascularization.

The HG + hEOs treatment restores endometrial thickness and glandular density to physiological levels

The analysis of endometrial parameters revealed notable findings regarding endometrial thickness and gland concentration between groups (Fig. 3A and E). The total endometrial thickness of PBS (0.30 ± 0.04 mm) and HG (0.31 ± 0.02 mm) conditions were statistically lower compared to the SHAM group (0.40 ± 0.04 mm) ($p = 0.028$ and $p = 0.026$, respectively). Remarkably, no differences were observed between the total endometrial thickness of HG + hEOs (0.37 ± 0.016 mm) and SHAM (0.40 ± 0.04 mm) groups.

Interestingly, no significant differences were detected in the luminal epithelial thickness across any of the conditions (Fig. 3A and F). Given that the stroma constitutes the main component of the endometrium, it was anticipated that stromal thickness would exhibit a similar statistical pattern to the overall endometrial thickness. Consistent with this expectation, no significant differences were found between the SHAM (0.38 ± 0.08 mm) and HG + hEOs (0.35 ± 0.04 mm) groups. However, the stromal thickness in the PBS (0.29 ± 0.07 mm) and HG (0.27 ± 0.04 mm) conditions was significantly lower compared to the SHAM group ($p = 0.028$ and $p = 0.008$, respectively) (Fig. 3G). Additionally, the stromal thickness in the HG + hEOs condition was significantly higher than that in the HG group ($p = 0.037$).

Regarding the endometrial gland concentration, no significant differences were observed between SHAM, PBS, and HG + hEOs groups (Fig. 3A and H). However, it was significantly higher in the HG + hEOs group (43.96 ± 5.41 glands per mm^2) compared to the HG condition (22.89 ± 1.73 glands per mm^2), indicating a superior regenerative effect than the hydrogel treatment alone ($p = 0.004$).

These findings indicate that only the complete treatment (HG + hEOs) was able to restore endometrial structure, including stromal thickness and gland concentration, to levels comparable to the SHAM control condition.

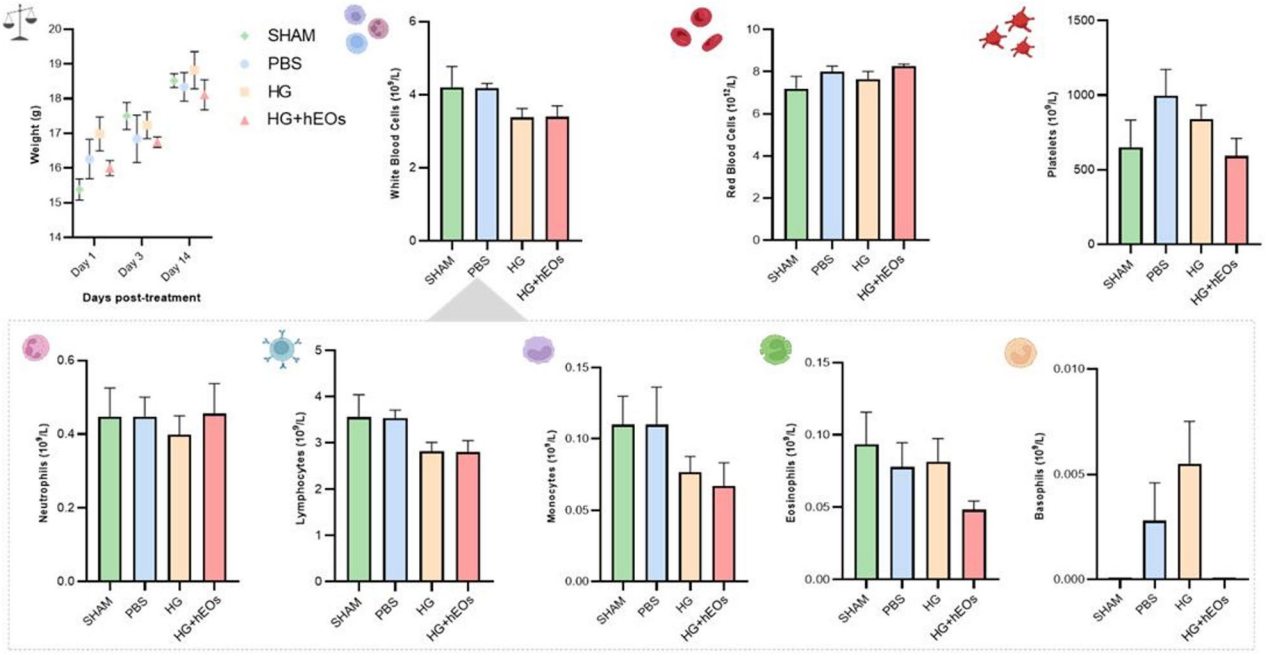

	WBC (10^9/L)	NEUT (10^9/L)	LYMPH (10^9/L)	MONO (10^9/L)	EOS (10^9/L)	BASO (10^9/L)	RBC (10^{12}/L)	PLT (10^9/L)
SHAM	4.205 ± 1.393	0.446 ± 0.192	3.555 ± 1.185	0.11 ± 0.05	0.09 ± 0.05	0 ± 0	7.191 ± 1.431	649.5 ± 449.704
PBS	4.178 ± 0.512	0.448 ± 0.112	3.54 ± 0.537	0.11 ± 0.05	0.08 ± 0.04	0.002 ± 0.005	7.98 ± 1.031	995.4 ± 354.685
HG	3.376 ± 0.606	0.298 ± 0.125	2.815 ± 0.467	0.08 ± 0.03	0.08 ± 0.04	0.005 ± 0.005	7.63 ± 0.946	840.5 ± 226.647
HG+hEOs	3.395 ± 0.846	0.455 ± 0.181	2.806 ± 0.697	0.17 ± 0.05	0.07 ± 0.05	0.001 ± 0.004	8.269 ± 0.259	592.142 ± 320.173

Fig. 2 Body weight monitoring and haematological analysis after treatment. Graphical representation of the body weight (on days 1, 3 and 14 post-treatment) and haematocrit values (on day 14 post-treatment) of mice from the endometrial regeneration group ($n = 25$). No significant differences were observed between groups, neither in the body weight nor in blood parameters, confirming the biocompatibility of both treatments. Data are presented as mean ± SEM. *WBC* White Blood Cells, *NEUT* Neutrophils, *LYMPH* Lymphocytes, *MONO* Monocytes, *EOS* Eosinophils, *BASO* Basophils, *RBC* Red Blood Cells, *PLT* Platelets

The HG + hEOs treatment reduces fibrosis and ferroptosis while supporting cell proliferation and neovascularization in damaged endometrium

Given the critical role of fibrosis in the pathophysiology of AS/EA/TE, endometrial collagen deposition was quantified to assess fibrotic changes across experimental groups. As expected, the PBS group exhibited significantly higher fibrosis levels (30.17 ± 11.43%) compared to the SHAM condition (12.74 ± 1.57%), validating the robustness of the induced injury model ($p = 0.012$). Hydrogel-based treatments did not significantly improve deposition of collagen fibers. In contrast, fibrotic area was significantly reduced in the HG (13.77 ± 0.81%) and HG + hEOs (9.87 ± 1.83%) groups compared to the PBS condition ($p = 0.017$ and $p = 0.008$, respectively), with values closely resembling those of the SHAM group (Fig. 3B and I). In line with these findings, the PBS group exhibited a significantly higher percentage of Fe^{3+}positive area (0.32 ± 0.29%) compared to the other conditions (0.002 ± 0.002%, 0.03 ± 0.06%, 0.003 ± 0.004% for SHAM, HG and HG + hEOs, respectively) ($p = 0.013$, $p = 0.028$, $p = 0.014$) (Supplementary Figure S1). These results are indicative of elevated levels of ferroptosis, which is an iron-dependent form of cell death. Taken together, both HG and HG + hEOs treatments effectively mitigate endometrial fibrosis and cell death, restoring tissue architecture to near-physiological levels.

Cell proliferation analysis revealed no statistically significant differences between groups, indicating similar levels of proliferation rates across conditions (Fig. 3C and J). As will be discussed later, this outcome may be related to the timing of the analysis, as proliferative activity could have peaked earlier in the regenerative process.

Finally, we assessed blood vessel density in terms of both total vessels (vascularization) and newly formed vessels (neovascularization) across experimental conditions. Regarding vascularization, the PBS group exhibited a significantly reduced vessel density (3.91 ± 2.29%) compared to the SHAM condition (16.68 ± 4.20%) ($p = 0.007$), reflecting impaired vascularization following injury (Fig. 3D and K). Similarly, neovascularization showed a comparable trend, with significantly lower

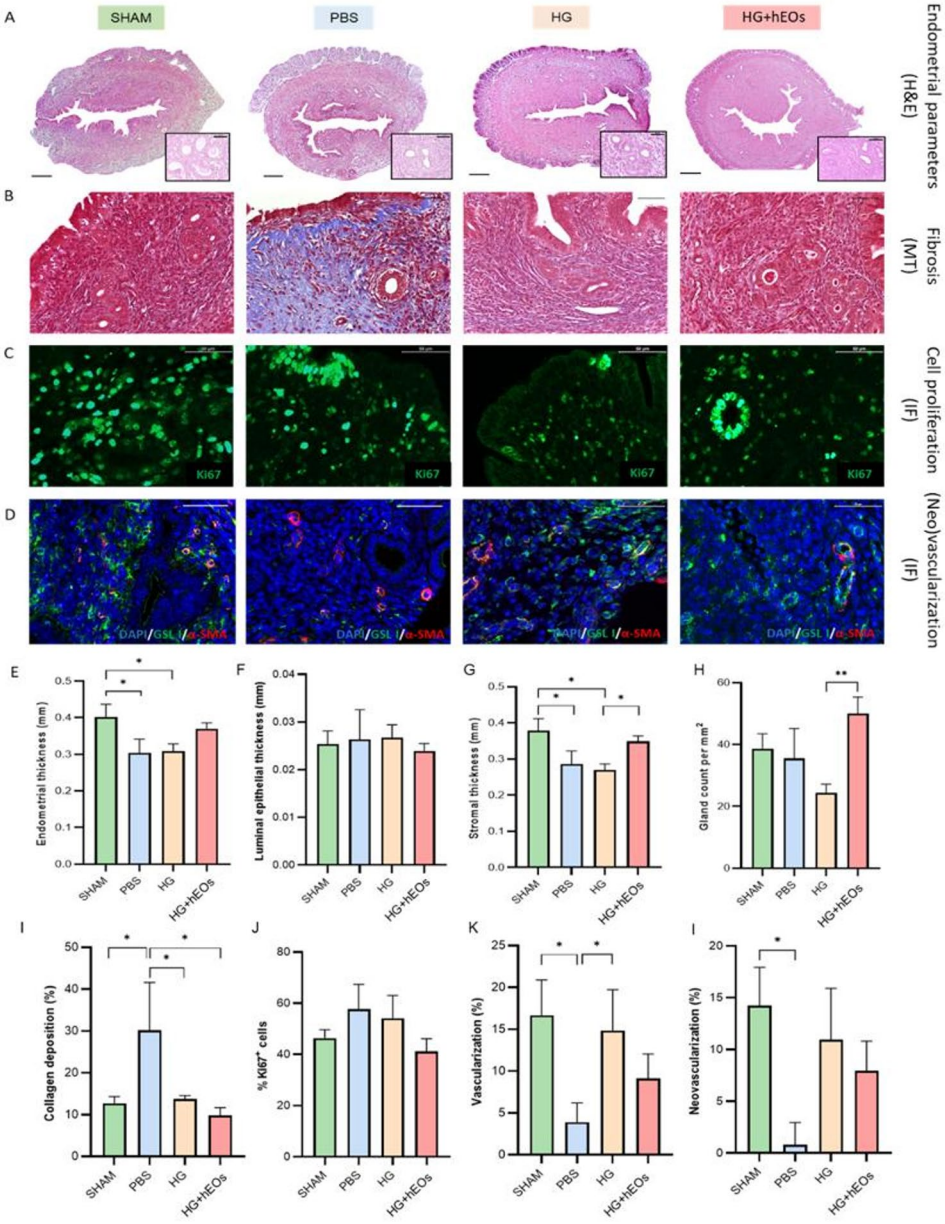

Fig. 3 Endometrial regeneration at histological level. Representative cross-sections of uterine tissue from SHAM, PBS, HG, and HG + hEOs groups. **A** H&E showing endometrial thickness and gland concentration; **B** Masson's Trichrome staining representing endometrial fibrosis; **C** Immunofluorescence of Ki67 marker for cell proliferation; **D** Double immunofluorescence for α–SMA and GSL-I, showing (neo)vascularization; **E**–**L** Graphical representation and quantification of the endometrial parameters. Scale bars = 50 µm. Data are presented as mean ± SEM. *$p < 0.05$, **$p < 0.01$. *H&E* Hematoxylin and eosin, *MT* Masson's Trichrome, *IF* immunofluorescence, *HG* PM + EndoECM hydrogel, *hEOs* Human endometrial organoids

levels observed in the PBS group (0.80 ± 2.16%) relative to the SHAM group (14.22 ± 3.69%) ($p = 0.006$) (Fig. 3D and L). Both HG and HG + hEOs treatments resulted in a substantial recovery of blood vessel density, including both new and mature vessels, with values closely resembling those of the SHAM group. These findings suggest that both treatments effectively enhance neovascularization, potentially contributing to the restoration of normal vascular architecture in the endometrial tissue.

The HG + hEOs treatment modulates molecular pathways toward endometrial repair and immune balance

To validate our histological findings, we performed RNA sequencing of murine endometrial tissue followed by GSEA. Functional enrichment was assessed based on Gene Ontology (GO: Biological Process, Cellular Component, Molecular Function) and Kyoto Encyclopedia of Genes and Genomes (KEGG) terms (Supplementary Table 1). All raw sequencing data are available through

the Gene Expression Omnibus (GEO) under accession number GSE304635. When comparing each condition to SHAM group, we identified 633, 552, and 507 differentially enriched pathways in PBS, HG, and HG + hEOs groups, respectively (Supplementary Figure S2). Notably, the HG + hEOs vs. SHAM comparison revealed the lowest number of altered pathways, suggesting that combined treatment with HG + hEOs restores the transcriptomic profile of damaged endometria toward a state more similar to healthy tissue.

To further explore the molecular impact of tissue injury and treatment, we focused on the differentially enriched Biological Processes (BP) in comparisons against the damaged model (PBS group) (Supplementary Figure S2). In the SHAM vs. PBS comparison, 529 enriched BP included pathways associated with immune activation, tissue remodelling, and cell apoptosis, confirming that the PBS condition reflects a disrupted endometrial environment (Fig. 4A). In contrast, HG treatment alone (HG vs. PBS comparison) induced 422 BP related to epithelial cell proliferation, angiogenesis, and hormone signalling, while also showing signs of local immune activation (Fig. 4B). Importantly, HG + hEOs vs. PBS comparison resulted in 429 differentially expressed BP terms, which were grouped into functional categories to facilitate biological interpretation (Fig. 4C). Regenerative processes such as angiogenesis, vascularization, cell proliferation, and regenerative and inflammatory immune response were upregulated. In contrast, fibrosis-related pathways were downregulated, suggesting that HG + hEOs not only promotes tissue repair but also attenuates collagen deposition.



Fig. 4 Gene Set Enrichment Analysis (GSEA) following RNA sequencing. **A**, **B** GSEA plots showing selected representative biological processes (BP) that were significantly enriched in the SHAM vs. PBS (**A**), HG vs. PBS (**B**), and HG + hEOs vs. PBS (**C**) comparisons. Both upregulated (green) and downregulated (red) terms are shown, with bar length indicating significance ($-\log_{10}$ (p-value)) and dot size representing the number of genes associated with each term. **C** also includes a summary of the 429 differentially expressed BP pathways in the HG + hEOs vs. PBS comparison, which were grouped into major functional categories (angiogenesis and vascularization, cell proliferation, negative and positive immune response, and fibrosis). Green and red sections indicate up- and downregulated functions in HG + hEOs, respectively

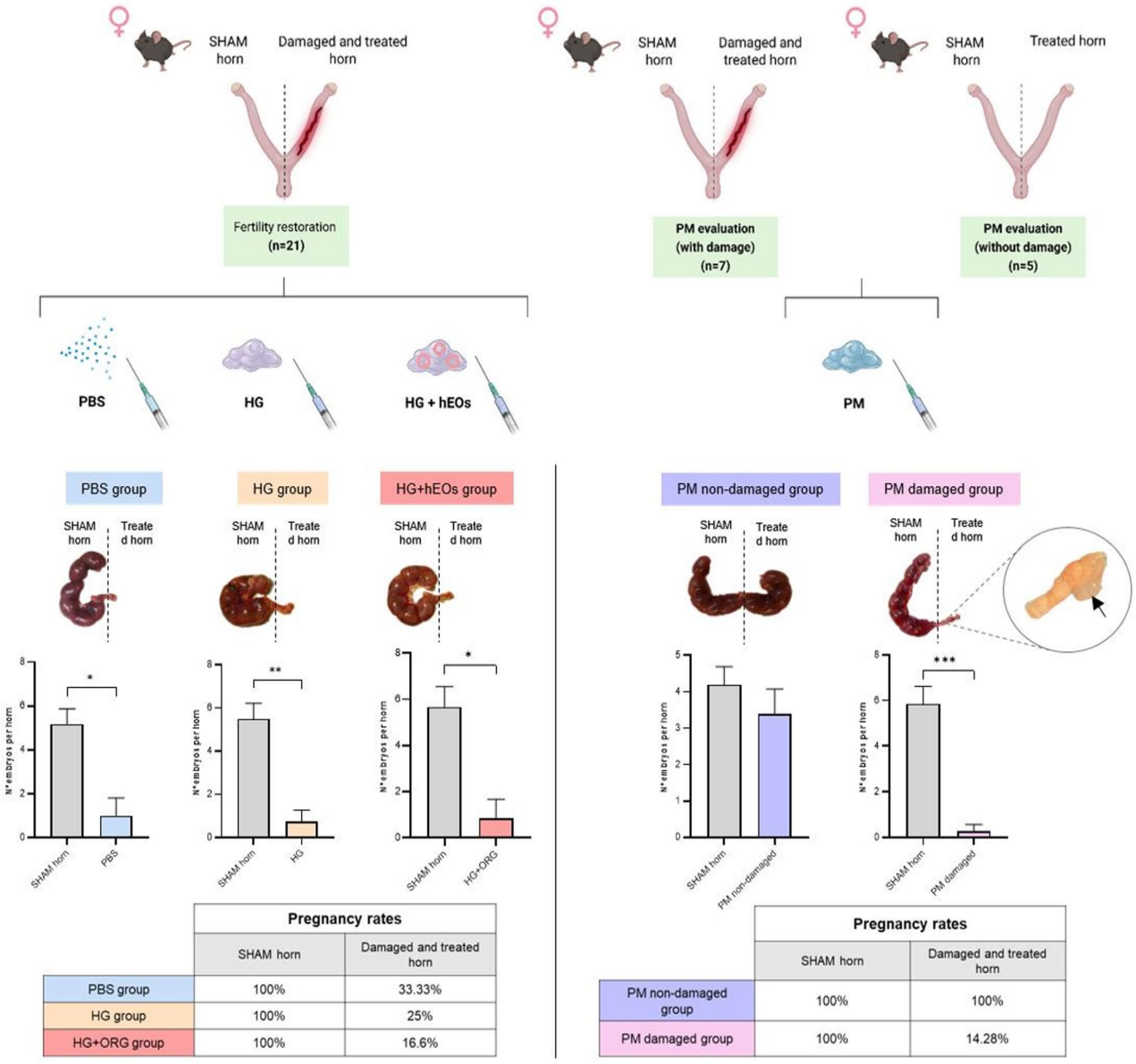

Fig. 5 Evaluation of fertility restoration after treatment. **A** Representative images of uterine horns from HG + hEOs, HG, and PBS groups, together with the statistical data of the pregnancy rates and embryo count. Neither HG nor HG + hEOs treatments was able to restore the fertility of the animal model. **B** Representative images of uterine horns from non-damaged and damaged mice both treated with PM alone, together with the statistical analyses of fertility outcomes. PM only impact in fertility when mice were previously damaged. In both cases, each animal had one SHAM (non-damaged) horn and one damaged and treated horn. Data are presented as mean ± SEM. *$p < 0.05$

Endometrial regeneration does not translate into fertility restoration: puramatrix may impair implantation due to prolonged retention

Once endometrial regeneration was confirmed, we assessed the recovery of endometrial functionality by evaluating pregnancy outcomes. Pregnancy rates were calculated as the number of pregnant horns divided by the total number of horns per group, considering that each animal had one control horn and one damaged and treated horn. In the control horns of the PBS, HG, and HG + hEOs groups, the pregnancy rate was 100% (6/6, 8/8, and 6/6, respectively). However, pregnancy rates in the treated horns were 25% (2/8) in the HG group and 16.67% (1/6) in the HG + hEOs group, showing no substantial improvement over the 33.33% (2/6) of the PBS condition (Fig. 5A). Consistently, the number of embryos per horn followed the same pattern. While SHAM horns across all groups exhibited high embryo counts (5.17 ± 0.7 embryos, 5.5 ± 0.73 embryos, and 5.67 ± 0.83 embryos in PBS, HG, and HG + hEOs, respectively), the treated horns showed a significantly reduced number of embryos (1 ± 0.82 embryos, 0.75 ± 0.53 embryos, and 0.83 ± 0.83

in PBS, HG, and HG + hEOs; $p = 0.03$, $p = 0.004$, $p = 0.03$, respectively). Importantly, neither HG nor HG + hEOs treatments were able to restore embryo numbers to control levels, with embryo counts remaining low and comparable to the PBS group (Fig. 5A). These findings suggest that, despite promoting endometrial regeneration, none of the treatments were sufficient to restore fertility in the AS/EA/TE model.

To further investigate the impact of this treatment on fertility, we conducted an additional animal model with two experimental groups: PM non-damaged and PM-damaged mice. As PM is the exclusive component common to both the HG and HG + hEOs groups, we wanted to isolate its effect in the context of fertility, which has not been studied before. The PM non-damaged group showed no impairment in fertility, as pregnancy rates were 100% (6/6) in both treated and control horns, indicating that PM alone does not negatively affect fertility. However, fertility was significantly affected in the PM-damaged group, where the gestational rate was 14.30% (1/7) in treated horns, compared to the 100% (7/7) in the control horns. Similarly, the number of embryos per horn followed the same trend. SHAM horns in both conditions exhibited high embryo counts (4.2 ± 0.49 embryos and 5.85 ± 0.77 embryos in PM non-damaged and PM damaged mice, respectively), but only the treated horns from the PM-damaged condition showed a significantly reduced number of embryos (0.29 ± 0.29 embryos, $p = 0.0003$). No significant differences were observed in the number of embryos between the SHAM and treated horns from the PM-non-damaged group (3.4 ± 0.68) (Fig. 5B). In addition, we observed macroscopic alterations exclusively in the damaged uterine horns after PM treatment, which can be attributed to the prolonged retention of PM in the endometrial tissue (Fig. 5B). These results suggest that while PM may have an impact on fertility, its effects are dependent on the presence of endometrial damage, emphasizing the need for careful consideration when using PM as a treatment in regenerative therapies for the endometrium.

Discussion

Regenerative medicine has revolutionized the field of reproductive biology, offering novel approaches for the treatment of endometrial pathologies that compromise fertility, such as AS, EA, or TE. Among these, bioengineering and cell-based therapies have emerged as promising strategies for promoting endometrial regeneration [4]. However, when used separately, each of these approaches presents certain limitations. Whereas hydrogels lack the cellular components necessary for full tissue restoration, cell-based treatments require a supportive microenvironment to ensure functional integration and avoid rapid biodegradation [14, 31]. Since organoid transplantation overcome conventional cell therapy in terms of lifespan and cryopreservation [15, 20, 32], this study propose a synergic treatment based on the combination of hEOs with a hybrid endometrial-derived hydrogel to promote tissue regeneration in an AS/EA/TE animal model.

Despite the human origin of the injected cells into immunocompetent mice, no systemic signs of immune rejection were observed. The biocompatibility of the HG was demonstrated in previous experiments [10] ensuring a favourable microenvironment for cell integration. Additionally, hEOs are composed of glandular progenitor epithelial cells that express stem markers such as SSEA-1 [14, 33] and CD44 [17], with their expression increasing during in vitro expansion. In this study, hEOs were utilized at late passages (passage 15), resulting in a higher proportion of progenitor cells, which may contribute to enhancing their immune tolerance in the animal model. In addition, this population can proliferate selectively in response to endometrial repair, contributing to the re-epithelialization of the uterine surface after menses [34]. Thus, the low immunogenicity and the regenerative capacity of hEOs make them a strong candidate for allogeneic cell therapy, similarly to other endometrial progenitor cell-based therapies [35].

Beyond confirming the biocompatibility of the treatment, histological analyses of murine endometrium also demonstrated its regenerative potential. Under AS/EA/TE conditions, the endometrium becomes thin and fibrotic [36], accompanied by a reduced number of endometrial glands and blood vessels [37]. Given these pathological features, we focused our analysis on typical endometrial parameters evaluated in previous similar studies [14–16, 21]. First, endometrial thickness was significantly restored following the complete treatment (HG + hEOs), reaching levels comparable to the control condition. This recovery was primarily driven by an increase in stromal thickness, while epithelial thickness remained similar across groups. Although the luminal epithelium was largely preserved in the animal model, in contrast to classical descriptions of AS where epithelial denudation is often observed [38], we have also detected the expression of typical fibrotic markers (such as collagen deposition or Masson's trichrome [16]), suggesting that the model shares key histopathological features with AS, EA, and TE conditions. Since the stroma serves as the structural framework for endometrial glands and blood vessels, its thickness restoration is particularly relevant for re-establishing the endometrial function [39]. In addition, stromal fibrosis was significantly reduced after the complete treatment, leading to the recovery of endometrial gland count and blood vessel formation to levels comparable to those observed in control conditions. Interestingly, iron deposition was mainly detected in the non-treated group,

consistent with the involvement of ferroptosis in fibrosis progression [40]. Given that ferroptosis is an iron-dependent form of cell death implicated in fibrotic processes across multiple conditions, including ovarian endometrioma and intrauterine adhesions [41, 42], its reduction following treatment further supports the regenerative effects previously observed. Regarding cell proliferation, no significant differences were detected between experimental groups. This result could be explained because of the timing of our histological analysis (14 days). Similar studies on organoid transplantation have reported the most pronounced differences in cell proliferation rates at 3–4 weeks post-transplantation [15, 17], a time frame that aligns with the transition from inflammation to proliferation during tissue healing [43]. Future investigations should consider extended evaluation periods to capture significant differences in proliferative responses. Finally, both HG and HG + hEOs treatments resulted in a substantial recovery of neovascularization in the AS/EA/TE animal model, a crucial step in the restoration of the endometrial microenvironment [44, 45]. In particular, the generation of new blood vessels is critical for stromal cell migration and glandular regeneration via vascular endothelial growth factor (VEGF) signalling, and also complements the function of pre-existing vasculature by improving local metabolic support [46].

Of note, the transcriptomic analysis further supports our histological findings by providing molecular evidence of endometrial damage and subsequent tissue regeneration following treatment. Compared to the SHAM group, the fibrosis and reduced endometrial thickness observed histologically in the PBS condition were mirrored at the molecular level by the upregulation of collagen deposition and apoptosis, together with the downregulation of cell cycle and division. Interestingly, despite the absence of systemic alterations in haematological tests, GSEA revealed a localized inflammatory immune response triggered by ethanol injury. This local reaction reflects the immune imbalance of AS/EA/TE patients, which actually contributes to their impaired endometrial microenvironment and infertility [38, 47]. As expected, this inflammatory immune response was upregulated in the murine endometrium of the HG and HG + hEOs treatments when compared to PBS. This response reflects the physiological reaction of our immunocompetent AS/EA/TE model to the introduction of exogenous therapeutic components, which naturally trigger a controlled local immune response to maintain tissue integrity. However, GSEA also identified a concurrent activation of a regenerative immune response exclusively in the HG + hEOs vs. PBS comparison, mainly associated with tissue remodelling and repair. The positive regulation of anti-inflammatory cytokines (IL-4, IL-10), together with the negative regulation of pro-inflammatory factors (IL-1β, IL-6) suggest in an immune microenvironment that promotes the polarization of M1 to M2 macrophages [48]. This process is particularly relevant in AS patients, where IL-4-induced M2 macrophages can significantly reduce fibrosis in endometrial stromal cells [49]. In addition, the presence of $CD4^+$ T cells within this cytokine profile suggests the activation of T-helper 2 and T-regulatory lymphocytes, which are known to increase following cell-based therapies for AS and TE conditions [50]. Moreover, transcriptomic data from the HG + hEOs vs. PBS comparison also revealed the upregulation of angiogenesis (i.e. VEGF production) and cell proliferation of epithelial and endothelial cells, suggesting a mechanistic explanation for the endometrial restoration observed in our previous histological analyses. Taken together, these results show that HG + hEOs treatment promotes a regenerative environment that helps restore a more normal endometrial transcriptomic profile, even in the presence of an initial inflammatory immune response.

Although histological and molecular analyses confirmed a significant improvement in endometrial architecture and regeneration, these structural changes did not translate into successful fertility restoration. Pregnancy rates and embryo count remained low across treated groups, similarly to non-treated animals. However, no alterations related to embryo implantation and development were reported after molecular analyses. Given that both treated groups shared the HG based on PM + EndoECM, we focused on this component as the key contributor to the observed effects.

The EndoECM component of the hybrid hydrogel was discarded as a potential negative factor for fertility, as previous studies have demonstrated that it serves as a beneficial biological carrier and is fully absorbed within 14 days of injection in the uterus [16, 21]. Because of this, we evaluated whether PM alone still persist at this time point. Surprisingly, our additional experiments with PM alone showed a significant negative impact on fertility, but only when combined with endometrial injury. In a damaged uterus, the native ECM is often deficient or disorganized due to the inflammatory response triggered by tissue injury [51]. If a high viscous hydrogel such as PM is injected, it may occupy physical space within the uterine cavity, forming a barrier that physically blocks the embryo attachment to the endometrial epithelium [52]. In addition, the thixotropic and rheological properties of the PM formulation enhance the retention of $RADA_{16}$ peptides at the wound site and also difficult their enzymatic degradation [10, 53]. As a result, we observed macroscopic uterine alterations in the damaged uterine horns after PM treatment, which negatively impact on embryo implantation by distorting the cavity or creating physical obstructions, similarly to uterine fibroids or polyps [54]. Future studies should investigate whether extending the

recovery period before mating –until complete reabsorption of the HG in the uterus– improves reproductive outcomes.

Despite the limitations of HG in fertility restoration, our histological analyses confirm that its biological activity positively impacts endometrial regeneration in damaged tissue. However, this regenerative effect is more pronounced when combined with hEOs. Although the specific mechanism of action of hEOs was not investigated in this study, we propose that the therapeutic effect of hEO-derived cells is primarily mediated by the secretion of paracrine factors. According to this hypothesis, these progenitor cells release various biomolecules, including growth factors, angiogenic and immunosuppressive factors, chemokines, and exosomes, all of which contribute to tissue regeneration [55, 56]. Of note, this study is pioneering in the use of hEOs in an immunocompetent murine model. Despite the different origin of donor and recipient, this organoid therapy has demonstrated its immunomodulatory and regenerative properties, unveiling new strategies for endometrial repair even in allogeneic settings.

Conclusions

In conclusion, this study demonstrates that the combination of a hybrid endometrial-derived hydrogel (PM + EndoECM) with hEOs promotes endometrial regeneration in an immunocompetent murine model of AS/EA/TE. This dual treatment restored endometrial parameters, increased angiogenesis, and reduced fibrosis and ferroptosis, while promoting a regenerative immune microenvironment at the molecular level. Further investigation is needed to optimize the duration of the hydrogel use to fully unlock the reproductive potential of this allogeneic regenerative therapy.

Abbreviations

AS	Asherman syndrome
BASO	Basophils
BP	Biological processes
cDNA	Complementary DNA
dUTP	Deoxyuridine triphospate
EA	Endometrial atrophy
EndoECM	Endometrial extracellular matrix
EOS	Eosinophils
EtOH	Ethanol
ExM	Expansion medium
GEO	Gene expression omnibus
GLS I	Griffonia simplicifolia lectin I
GO	Gene ontology
GSEA	Gene set enrichment analysis
hEOs	Human epithelial endometrial organoids
H&E	Haematoxylin and eosin
HG	Hybrid hydrogel
IF	Immunofluorescence
KEGG	Kyoto encyclopaedia of genes and genomes
LYMPH	Lymphocytes
MONO	Monocytes
MT	Masson's trichrome staining
NEUT	Neutrophils
PB	Prussian blue
PCA	Principal component analysis
PCR	Polymerase chain reaction
PLT	Platelets
PM	PuraMatrix
RBC	Red Blood Cells
RT	Room temperature
SEM	Standard error of the mean
TE	Thin endometrium
VEGF	Vascular endotelial growth factor
VST	Variance-stabilized transformed
WBC	White blood cells
α-SMA	Alpha-smooth muscle actin

Supplementary Information

The online version contains supplementary material available at https://doi.org/10.1186/s13287-026-04900-1.

Supplementary material 1.

Supplementary material 2.

Supplementary material 3.

Acknowledgements

The authors declare that they have not used AI-generated work in this manuscript.

Author contributions

Conception of the work: M.G.-Á., C.B.-F., I.C., and A.P.; design of the work: M.G.-Á., C.B.-F., A.D., and I.C.; acquisition, analysis, and interpretation of data: M.G.-Á., E.F.-H., M.A.-H., C.B.-F., P.A.-F., N.C., and A.F.; manuscript and figure preparation: M.G.-Á. and C.B.-F.; manuscript review: I.C., E.F.-H., M.A.-H., C.B.-F., P.A.-F., N.C., H.F. and A.P. All authors approve the submitted version and agree both to be personally accountable for the author's own contributions, and to ensure that questions related to the accuracy or integrity of any part of the work are appropriately investigated, resolved, and the resolution documented in the literature.

Funding

This research was funded by the Instituto de Salud Carlos III (ISCIII) thought the project "PI21/00305", and co-funded by the European Union (Fondo Social Europeo), «El FSE invierte en tu futuro» through the Miguel Servet Program (CP20/00120 [H.F.] and CP19/00149 [I.C.]), Spanish Ministry of Science, Innovation, and Universities (FPU20/00251 [M.G.-Á.], FPU23/01831 [M.A.-H.], CNS2024-154767 [C.B-F. and I.C.]), the Generalitat Valenciana (CIPROM/2021/058 [P.A.-F., E.F.-H., A.P., and I.C.]) and by the MICIU/AEI/https://doi.org/10.13039/501100011033 and FSE+ (PID2024-163068OB-I00 [I.C.]).

Data availability

The datasets used and/or analyzed during the current study are available from the corresponding author on reasonable request. All raw sequencing data are available through the Gene Expression Omnibus (GEO) under accession number GSE304635.

Declarations

Ethics approval and consent to participate

Animal experiments executed in this study were approved by the ethical committee of the Universitat de Valencia and the Generalitat Valenciana (2024-VSC-PEA-0110, 2024-VSC-PEA-0225). All animal procedures complied with Directive 2010/63/EU. The approved project was entitled "Uso de organoides endometriales humanos como componentes regenerativos en un modelo murino con Síndrome de Asherman" and received approval on April 29, 2024. The use of human-derived samples was also approved by the Ethical Committee of the Hospital Universitari I Politècnic La Fe (2021-162-1, Valencia, Spain) and conducted in accordance with the institutional and international guidelines for the use of human-derived samples. All participants provided written informed consent for participation in the study and the use of their samples, in accordance with current ethical and legal regulations. The

approved project was entitled "Human organoids to model the healthy female reproductive tract using native bioengineering supports and their pre-clinical applications in the gynecological medicine field" and received approval on April 25, 2024.

Consent for publication
All authors agree to the publication of this work.

Competing interests
The authors declare no competing interests.

Author details
[1]IVIRMA Global Research Alliance, IVI Foundation, Instituto de Investigación Sanitaria La Fe (IIS La Fe), Valencia, Spain
[2]Universitat de València, Valencia, Spain
[3]IVIRMA Global Research Alliance, IVIRMA Rome, Roma, Italy

Received: 19 September 2025 / Accepted: 2 January 2026
Published online: 13 January 2026

References

1. de Miguel-Gómez L, López-Martínez S, Francés-Herrero E, Rodríguez-Eguren A, Pellicer A, Cervelló I. Stem cells and the endometrium: from the discovery of adult stem cells to Pre-Clinical models. Cells 8 De Marzo De. 2021;10(3):595.
2. Cervelló I, Mas A, Gil-Sanchis C, Simón C. Somatic stem cells in the human endometrium. Semin Reprod Med Enero De. 2013;31(1):69–76.
3. de Miguel-Gómez L, Romeu M, Pellicer A, Cervelló I. Strategies for managing asherman's syndrome and endometrial atrophy: since the classical experimental models to the new bioengineering approach. Mol Reprod Dev Agosto De. 2021;88(8):527–43.
4. Rodríguez-Eguren A, Bueno-Fernandez C, Gómez-Álvarez M, Francés-Herrero E, Pellicer A, Bellver J et al. Evolution of biotechnological advances and regenerative therapies for endometrial disorders: a systematic review. Hum Reprod Update. 25 de mayo de 2024;dmae013.
5. Gómez-Álvarez M, Agustina-Hernández M, Francés-Herrero E, Rodríguez-Eguren A, Bueno-Fernandez C, Cervelló I. Addressing key questions in organoid models: Who, Where, How, and why? Int J Mol Sci 6 De Noviembre De. 2023;24(21):16014.
6. Francés-Herrero E, Rodríguez-Eguren A, Gómez-Álvarez M, de Miguel-Gómez L, Ferrero H, Cervelló I. Future challenges and opportunities of extracellular matrix hydrogels in female reproductive medicine. Int J Mol Sci 29 De Marzo De. 2022;23(7):3765.
7. Zeraatpisheh Z, Mirzaei E, Nami M, Alipour H, Mahdavipour M, Sarkoohi P, et al. Local delivery of Fingolimod through PLGA nanoparticles and PuraMatrix-embedded neural precursor cells promote motor function recovery and tissue repair in spinal cord injury. Eur J Neurosci Agosto De. 2021;54(4):5620–37.
8. Wang R, Wang Z, Guo Y, Li H, Chen Z. Design of a RADA16-based self-assembling peptide nanofiber scaffold for biomedical applications. J Biomaterials Sci Polym Ed 13 De Junio De. 2019;30(9):713–36.
9. Yao X, Hu,Yicun L et al. Maoqiang, Peng, Kaichen, Wang, Peng, Gao, Yanbing, Self-Assembling Peptide RADA16: A Promising Scaffold for Tissue Engineering and Regenerative Medicine. Nanomedicine. 1 de agosto de. 2023;18(19):1305-26.
10. Gómez-Álvarez M, Bueno-Fernandez C, Rodríguez-Eguren A, Francés-Herrero E, Agustina-Hernández M, Faus A et al. Hybrid Endometrial-Derived hydrogels: human organoid culture models and in vivo perspectives. Adv Healthc Mater. 20 de noviembre de 2023;e2303838.
11. Li Z, Zhao Y, Ouyang X, Yang Y, Chen Y, Luo Q, et al. Biomimetic hybrid hydrogel for hemostasis, adhesion prevention and promoting regeneration after partial liver resection. Bioact Mater Mayo De. 2022;11:41–51.
12. Ding X, Yu Y, Yang C, Wu D, Zhao Y. Multifunctional GO Hybrid Hydrogel Scaffolds for Wound Healing. Research (Wash D C). 2022;2022:9850743.
13. Chen M, Zhang Y, Xie Q, Zhang W, Pan X, Gu P, et al. Long-Term bone regeneration enabled by a polyhedral oligomeric Silsesquioxane (POSS)-Enhanced biodegradable hydrogel. ACS Biomater Sci Eng 9 De Septiembre De. 2019;5(9):4612–23.
14. Xu Y, Cai S, Wang Q, Cheng M, Hui X, Dzakah EE, et al. Multi-Lineage human endometrial organoids on acellular amniotic membrane for endometrium regeneration. Cell Transpl. 2023;32:9636897231218408.
15. Zhang H, Xu D, Li Y, Lan J, Zhu Y, Cao J, et al. Organoid transplantation can improve reproductive prognosis by promoting endometrial repair in mice. Int J Biol Sci. 2022;18(6):2627–38.
16. López-Martínez S, Rodríguez-Eguren A, de Miguel-Gómez L, Francés-Herrero E, Faus A, Díaz A, et al. Bioengineered endometrial hydrogels with growth factors promote tissue regeneration and restore fertility in murine models. Acta Biomater Noviembre De. 2021;135:113–25.
17. Hwang SY, Lee D, Lee G, Ahn J, Lee YG, Koo HS, et al. Endometrial organoids: a reservoir of functional mitochondria for uterine repair. Theranostics. 2024;14(3):954–72.
18. Aisenbrey EA, Murphy WL. Synthetic alternatives to matrigel. Nat Rev Mater Julio De. 2020;5(7):539–51.
19. López-Martínez S, Campo H, de Miguel-Gómez L, Faus A, Navarro AT, Díaz A et al. A natural xenogeneic endometrial extracellular matrix hydrogel toward improving current human in vitro models and future in vivo applications. Front Bioeng Biotechnol. 5 de marzo de 2021;9:639688.
20. Turco MY, Gardner L, Hughes J, Cindrova-Davies T, Gomez MJ, Farrell L, et al. Long-term, hormone-responsive organoid cultures of human endometrium in a chemically defined medium. Nat Cell Biol Mayo De. 2017;19(5):568–77.
21. Rodríguez-Eguren A, de Miguel-Gómez L, Francés-Herrero E, Gómez-Álvarez M, Faus A, Gómez-Cerdá M, et al. Human umbilical cord platelet-rich plasma to treat endometrial pathologies: methodology, composition and pre-clinical models. Hum Reprod Open. 2023;2023(1):hoac053.
22. Francés-Herrero E, Bueno-Fernandez C, Rodríguez-Eguren A, Gómez-Álvarez M, Faus A, Soto-Prado A et al. Growth factor-loaded ovarian extracellular matrix hydrogels promote in vivo ovarian niche regeneration and enhance fertility in premature ovarian insufficiency preclinical models. Acta Biomater. 15 de septiembre de 2024;186:125 – 40.
23. Ferrero H, Buigues A, Martínez J, Simón C, Pellicer A, Gómez R. A novel homologous model for noninvasive monitoring of endometriosis progression†. Biology Reprod 1 De Febrero De. 2017;96(2):302–12.
24. Bolger AM, Lohse M, Usadel B. Trimmomatic: a flexible trimmer for illumina sequence data. Bioinf 1 De Agosto De. 2014;30(15):2114–20.
25. Kim D, Paggi JM, Park C, Bennett C, Salzberg SL. Graph-based genome alignment and genotyping with HISAT2 and HISAT-genotype. Nat Biotechnol Agosto De. 2019;37(8):907–15.
26. Li H, Handsaker B, Wysoker A, Fennell T, Ruan J, Homer N, et al. The sequence Alignment/Map format and samtools. Bioinf 15 De Agosto De. 2009;25(16):2078–9.
27. Liao Y, Smyth GK, Shi W. FeatureCounts: an efficient general purpose program for assigning sequence reads to genomic features. Bioinf 1 De Abril De. 2014;30(7):923–30.
28. Love MI, Huber W, Anders S. Moderated Estimation of fold change and dispersion for RNA-seq data with DESeq2. Genome Biol. 2014;15(12):550.
29. Wu T, Hu E, Xu S, Chen M, Guo P, Dai Z et al. ClusterProfiler 4.0: A universal enrichment tool for interpreting omics data. Innov (Camb). 28 de agosto de 2021;2(3):100141.
30. ggplot2. Elegant Graphics for Data Analysis (3e) [Internet]. [citado 9 de mayo de 2025]. Disponible en: https://ggplot2-book.org/
31. Hu X, Wu H, Yong X, Wang Y, Yang S, Fan D, et al. Cyclical endometrial repair and regeneration: molecular mechanisms, diseases, and therapeutic interventions. MedComm. 2023;4(6):e425.
32. Boretto M, Cox B, Noben M, Hendriks N, Fassbender A, Roose H, et al. Development of organoids from mouse and human endometrium showing endometrial epithelium physiology and long-term expandability. Dev 15 De Mayo De. 2017;144(10):1775–86.
33. Francés-Herrero E, Juárez-Barber E, Campo H, López-Martínez S, de Miguel-Gómez L, Faus A et al. Improved Models of Human Endometrial Organoids Based on Hydrogels from Decellularized Endometrium. J Pers Med. 3 de junio de. 2021;11(6):504.
34. Kaitu'u-Lino TJ, Ye L, Gargett CE. Reepithelialization of the uterine surface arises from endometrial glands: evidence from a functional mouse model of breakdown and repair. Endocrinol 1 De Julio De. 2010;151(7):3386–95.
35. Gargett CE, Schwab KE, Deane JA. Endometrial stem/progenitor cells: the first 10 years. Hum Reprod Update 1 De Marzo De. 2016;22(2):137–63.
36. Liu D, Wang J, Zhao G, Jiang P, Song M, Ding H, et al. CSF1-associated decrease in endometrial macrophages May contribute to asherman's syndrome. Am J Reprod Immunol. 2020;83(1):e13191.
37. Dreisler E, Kjer JJ. Asherman's syndrome: current perspectives on diagnosis and management. Int J Womens Health. 2019;11:191–8.
38. Santamaria X, Roson B, Perez-Moraga R, Venkatesan N, Pardo-Figuerez M, Gonzalez-Fernandez J, et al. Decoding the endometrial niche of asherman's

syndrome at single-cell resolution. Nat Commun 21 De Septiembre De. 2023;14(1):5890.
39. Kirkwood PM, Shaw IW, Saunders PTK. Mechanisms of scarless repair at time of menstruation: insights from mouse models. Front Reprod Health. 2021;3:801843.
40. Langendonckt AV, Casanas-Roux F, Donnez J. Iron overload in the peritoneal cavity of women with pelvic endometriosis. Fertility Steril 1 De Octubre De. 2002;78(4):712–8.
41. Zhu Q, Yao S, Ye Z, Jiang P, Wang H, Zhang X et al. Ferroptosis contributes to endometrial fibrosis in intrauterine adhesions. Free Radic Biol Med 20 de agosto de 2023;205:151 – 62.
42. Zhang Y, Liu X, Deng M, Xu C, Zhang Y, Wu D, et al. Ferroptosis induced by iron overload promotes fibrosis in ovarian endometriosis and is related to subpopulations of endometrial stromal cells. Front Pharmacol 2 De Septiembre De. 2022;13:930614.
43. Landén NX, Li D, Ståhle M. Transition from inflammation to proliferation: a critical step during wound healing. Cell Mol Life Sci 14 De Mayo De. 2016;73(20):3861–85.
44. Alfer J, Happel L, Dittrich R, Beckmann MW, Hartmann A, Gaumann A, et al. Insufficient angiogenesis: cause of abnormally thin endometrium in subfertile patients? Geburtshilfe Frauenheilkd Julio De. 2017;77(7):756–64.
45. Chen Y, Chang Y, Yao S. Role of angiogenesis in endometrial repair of patients with severe intrauterine adhesion. Int J Clin Exp Pathol 15 De Junio De. 2013;6(7):1343–50.
46. Middelkoop MA, Don EE, Hehenkamp WJK, Polman NJ, Griffioen AW, Huirne JAF. Angiogenesis in abnormal uterine bleeding: a narrative review. Hum Reprod Update 28 De Febrero De. 2023;29(4):457–85.
47. Lv H, Zhao G, Jiang P, Wang H, Wang Z, Yao S et al. Deciphering the endometrial niche of human thin endometrium at single-cell resolution. Proceedings of the National Academy of Sciences. 22 de febrero de. 2022;119(8):e2115912119.
48. Chen S, Saeed AFUH, Liu Q, Jiang Q, Xu H, Xiao GG, et al. Macrophages in immunoregulation and therapeutics. Sig Transduct Target Ther 22 De Mayo De. 2023;8(1):1–35.
49. Feng D, Li Y, Zheng H, Wang Y, Deng J, Liu T, et al. IL-4-induced M2 macrophages inhibit fibrosis of endometrial stromal cells. Reprod Biol Junio De. 2024;24(2):100852.
50. Gharibeh N, Aghebati-Maleki L, Madani J, Pourakbari R, Yousefi M, Ahmadian Heris J. Cell-based therapy in thin endometrium and Asherman syndrome. Stem Cell Res Ther. 28 de enero de 2022;13:33.
51. Zehorai E, Gross Lev T, Shimshoni E, Hadas R, Adir I, Golani O, et al. Enhancing uterine receptivity for embryo implantation through controlled collagenase intervention. Life Sci Alliance 16 De Agosto De. 2024;7(10):e202402656.
52. Ma J, Gao W, Li D. Recurrent implantation failure: A comprehensive summary from etiology to treatment. Front Endocrinol (Lausanne). 5 de enero de 2023;13:1061766.
53. Gil ES, Aleksi E, Spirio L. PuraStat RADA16 Self-Assembling peptide reduces postoperative abdominal adhesion formation in a rabbit cecal sidewall injury model. Front Bioeng Biotechnol. 10 de diciembre de 2021;9:782224.
54. Horne AW, Critchley HOD. The effect of uterine fibroids on embryo implantation. Semin Reprod Med Noviembre De. 2007;25(6):483–9.
55. Osunkwo UA. Specificity of organoids for precision tissue regeneration: A review. Insights Stem Cell Res Therapy 24 De Abril De. 2021;3(1):003.
56. Jin H, Xue Z, Liu J, Ma B, Yang J, Lei L. Advancing organoid engineering for tissue regeneration and biofunctional reconstruction. Biomaterials Res 15 de abril de 2024;28:0016.

Publisher's Note

Springer Nature remains neutral with regard to jurisdictional claims in published maps and institutional affiliations.